JOC The Journal of Organic Chemistry

Article

pubs.acs.org/joc

Three Pyrene-Modified Nucleotides: Synthesis and Effects in Secondary Nucleic Acid Structures

Pawan Kumar, Khalil I. Shaikh, Anna S. Jørgensen, Surender Kumar,‡ and Poul Nielsen*

Nucleic Acid Center, Department of Physics, Chemistry and Pharmacy, University of Southern Denmark, 5230 Odense M, Denmark

Supporting Information

ABSTRACT: Synthesis of three pyrene-modified nucleosides was accomplished using the CuAAC reaction. Hereby, pyrene is attached either to the 5′-position of thymidine or to the 2′-position of 2′-deoxyuridine through triazolemethylene linkers, or to the 2′-position of 2′-deoxyuridine through a more rigid triazole linker. The three nucleosides were incorporated into oligonucleotides, and these were combined in different duplexes and other secondary structures, which were analyzed by thermal stability and fluorescence studies. The three monomers were found to have different impacts on the nucleic acid complexes. Hence, pyrene attached to the 5′-position shows a tendency for intercalation into the duplex as indicated by a general decrease in fluorescence intensity followed by an increase in duplex thermal stability. Pyrene attached to the 2′-position through a rigid triazole linker also shows a tendency for intercalation but with decrease in duplex stability, whereas the pyrene attached to the 2′-position through a triazolemethylene linker is primarily situated in the minor groove as indicated by an increase in fluorescence but here in most cases leading to increase in duplex stability. All three pyrene nucleotides lead to thermal stabilization of bulged duplexes and three-way junctions. In some cases when two pyrenes were introduced into the core of these complexes, the formation or disappearance of a fluorescence excimer band can be used to indicate the hybridization process. Hereby these oligonucleotides can act as specific recognition probes.

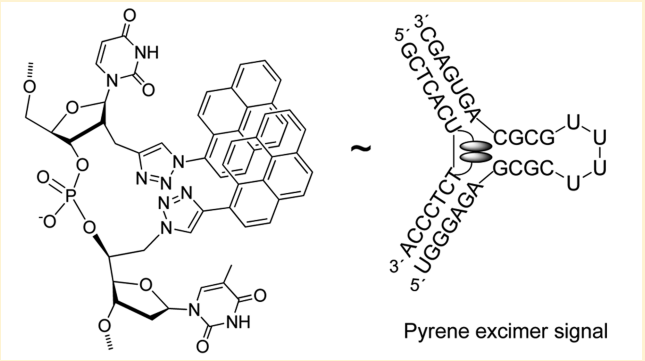

INTRODUCTION

The DNA double helix presents an excellent scaffold to attach various entities in an organized manner to find applications in diagnostics, DNA-mediated catalysis, nanotechnology, etc.[1,2] A series of nucleosides with additional nucleobases, commonly termed double-headed nucleosides, has been presented by us and others with the purpose of using the recognition potential of the additional nucleobases in various nucleic acid constructs.[3−8] Recently, we have shown that a 2′-deoxyuridine analogue (**A**) with an additional thymine in the 2′-position attached through a methylene linker (Figure 1) behaves as a compressed dinucleotide, recognizing nucleobases in the base pair ladder in the center of a Watson−Crick duplex.[6] On the other hand, the double-headed nucleoside monomer **B** with a methylene-linked thymine at the pro-*S* position of the C5′ carbon (Figure 1) when incorporated into an oligonucleotide can interact with the thymine of another nucleotide monomer **B** placed in the opposite strand in a so-called (−3) zipper arrangement via stacking in the minor groove.[3,4] The use of the Cu(I)-catalyzed alkyne azide cycloaddition (CuAAC) reaction[9] is well documented in the field of nucleoside/nucleic acid chemistry.[10,11] Recently, in our study of triazole stacking in the major groove leading to highly stable DNA:RNA duplexes, we have applied the CuAAC reaction to attach substituted and unsubstituted phenyl groups in the 5-position of the 2′-deoxyuridine and 2′-deoxycytidine.[12] We have also recently applied this reaction to attach an additional nucleobase in the study of a series of double-headed nucleosides (**C**-**H**) with an additional nucleobase or aromatic moiety in the pro-*S* position of the C5′-carbon of the thymidine (**C**-**F**)[4,5] and with an additional nucleobase (thymin-1-yl or adenin-9-yl) in the 2′-position of the 2′-deoxyuridine (**G** and **H**).[5] When incorporated into oligonucleotides and mixed with complementary unmodified oligonucleotides containing a central hairpin, **G** and **H** displayed stabilization of a three-way junction (TWJ) in both dsDNA and DNA:RNA contexts. Cross-strand stacking interactions between two additional bases from opposite strands were also observed in a so-called (+1) zipper motif for both **G** and **H**.[5]

Because of the environment-dependent fluorescence, pyrene-modified oligonucleotides have attracted considerable attention as fluorescent probes for the detection of hybridization to DNA/RNA complements.[13,14] Hence, hybridization can lead to modulation of the fluorescence intensity of the pyrene moieties. Pyrene in an electronically excited-state forms a π-stacking complex with a pyrene in the ground state when these two pyrenes are separated by ∼3.4 Å to give an excimer

Received: July 24, 2012
Published: October 8, 2012

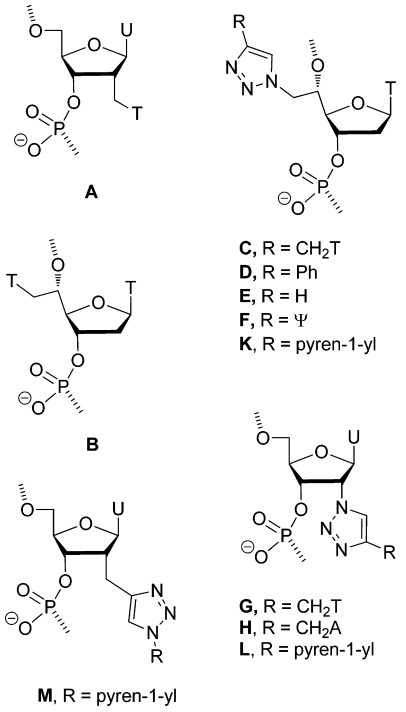

Figure 1. Double-headed nucleosides. U = uracil-1-yl, Ψ = uracil-5-yl, T = thymin-1-yl, A = adenin-9-yl.

fluorescence signal which is significantly red-shifted (with λ_{max} = ∼490 nm) relative to pyrene monomer fluorescence (with λ_{max} = ∼380−410 nm).[15] The pyrene excimer signal has been exploited for the detection of hybridization to DNA/RNA complements,[10,14,16] however not for the detection of secondary nucleic acids structures such as a TWJ. Nevertheless, pyrene-modified oligonucleotides have been used for the stabilization of TWJs.[17] In view of these observations, we decided to replace the additional nucleobases in **C** and **G** with pyrene, i.e., in the 2′-position of the 2′-deoxyuridine, and in the 5′(*S*)-*C*-position of the thymidine to investigate the stacking interactions from the larger aromatic surface area of pyrene and to study the effect of positioning pyrene at the branching point of a TWJ as well as in bulged dsDNA and DNA:RNA duplexes. Environment-dependent fluorescence properties of pyrene present an additional tool to get further insight into these interactions.

RESULTS AND DISCUSSION

Chemical Synthesis. The three nucleosides included in the present study were synthesized using the copper-catalyzed alkyne azide cycloaddition (CuAAC) reaction[9] (Scheme 1). Nucleoside **2** was synthesized by the reaction of commercially available 1-ethynylpyrene with appropriately protected 5′(*S*)-*C*-azidomethylthymidine **1**, which in turn was prepared by using our previously reported seven-step procedure from thymidine.[4] The reaction went smoothly by the use of standard conditions for the CuAAC reaction.[9] Desilylation of **2** using TBAF gave **3**, which on phosphitylation under standard conditions afforded the corresponding phosphoramidite **4** as an appropriate building block for automated oligonucleotide synthesis.

Uridine was converted in three high-yielding steps into the known intermediate 5′-*O*-dimethoxytrityl-2′-azido-2′-deoxyuridine **5**,[18] which was then reacted with 1-ethynylpyrene under the same CuAAC reaction conditions as before to give

Scheme 1[a]

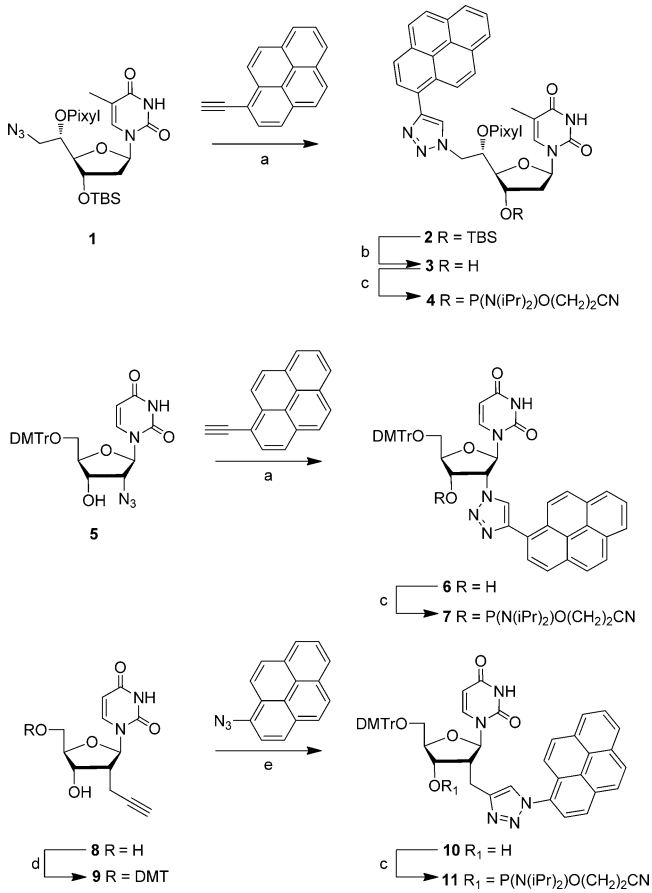

[a]Reagents and conditions: (a) $CuSO_4·5H_2O$, TBTA, Na ascorbate, THF:H_2O:pyridine (5:5:2 or 6:3:2, v/v/v), 84% **2**, 79% **6**. (b) TBAF, THF 82%. (c) $NC(CH_2)_2OP(N(i\text{-}Pr)_2)Cl$, $(i\text{-}Pr)_2NEt$, CH_2Cl_2, 69% **4**, 48% 7, 64% **11**. (d) DMTCl, pyridine, 79%. (e) $CuSO_4·5H_2O$, Na ascorbate, THF:H_2O:*t*-BuOH (3:1:1, v/v/v), 63%. TBTA = tris((1-benzyl-1,2,3-triazol-4-yl)methyl)amine. DMT = 4,4′-dimethoxytrityl.

nucleoside **6**. Subsequent phosphitylation of **6** afforded the phosphoramidite **7**, which can be used in standard automated solid-phase oligonucleotide synthesis.[19]

Recently, we have shown the six-step synthesis from uridine to the 2′-deoxy-2′-propargyluridine **8**.[20] This was reacted with 4,4′-dimethoxytrityl chloride in pyridine to afford the 5′-*O*-DMT-protected nucleoside **9**. Under CuAAC reaction conditions, **9** was reacted with 1-azidopyrene[21] to afford pyrene-modified nucleoside **10**. Phosphitylation of **10** afforded phosphoramidite **11**.

The three phosphoramidites **4**, **7**, and **11** were then introduced into oligonucleotides (ON's) to give the modified nucleotide monomers **K**, **L**, and **M** (Figure 1), respectively, by using standard solid-phase DNA synthesis with 1*H*-tetrazole as activator. Extended coupling time of 20 min was applied for the modified amidites, affording >80% coupling yields. The oligonucleotide (ON) sequences applied in this study are the same as used in former studies of zipper contacts in duplexes[3,4] (Table 1) and of bulged duplexes and TWJ's[3,7,22] (Tables 2 and 3).

Hybridization Studies. At first, an 11-mer duplex was studied, in which five centrally placed thymidines can be replaced systematically with the modified monomers (Table 1). One or two incorporation(s) of either of the monomers **K**, **L**,

dx.doi.org/10.1021/jo301571s | J. Org. Chem. 2012, 77, 9562−9573

Table 1. Hybridization Data for Modified Duplexes

entry	ON	duplex	zipper	T_m/°C,[a] (ΔT_m/°C[b]), [$\Delta\Delta T_m$/°C[c]]		
				X = K	**X = L**	**X = M**
1	**T1**	5′-d(CGC ATA TTC GC)-3′		45.5	45.5	45.5
	T2	3′-d(GCG TAT AAG CG)-5′				
2	**T1**	5′-d(CGC ATA TTC GC)-3′		45.5	37.0	45.5
	X1	3-′d(GCG **X**AT AAG CG)-5′		(0.0)	(−8.5)	(0.0)
3	**T1**	5′-d(CGC ATA TTC GC)-3′		45.5	45.5	50.5
	X2	3′-d(GCG TA**X** AAG CG)-5′		(0.0)	(0.0)	(+5.0)
4	**X3**	5′-d(CGC ATA T**X**C GC)-3′		47.0	38.5	43.5
	T2	3′-d(GCG TAT AAG CG)-5′		(+1.5)	(−7.0)	(−2.0)
5	**X4**	5′-d(CGC ATA **X**TC GC)-3′		45.5	41.0	46.5
	T2	3′-d(GCG TAT AAG CG)-5′		(0.0)	(−4.5)	(+1.0)
6	**X5**	5′-d(CGC A**X**A TTC GC)-3′		46.0	40.5	50.5
	T2	3′-d(GCG TAT AAG CG)-5′		(+0.5)	(−5.0)	(+5.0)
7	**T1**	5′-d(CGC ATA TTC GC)-3′		46.0	27.5	50.5
	X6	3′-d(GCG **X**A**X** AAG CG)-5′		(+0.5)	(−18.0)	(+5.0)
8	**X7**	5′-d(CGC A**X**A **X**TC GC)-3′		44.5	26.5	51.0
	T2	3′-d(GCG TAT AAG CG)-5′		(−1.0)	(−19.0)	(+5.5)
9	**X5**	5′-d(CGC A**X**A TTC GC)-3′	(+1)	53.0	33.5	39.5
	X2	3′-d(GCG TA**X** AAG CG)-5′		(+7.5) [+7.0]	(−12.0) [−6.5]	(−6.0) [−16.0]
10	**X5**	5′-d(CGC A**X**A TTC GC)-3′	(−1)	43.5	40.5	47.5
	X1	3′-d(GCG **X**AT AAG CG)-5′		(−2.0) [−2.5]	(−5.0) [+9.0]	(+2.0) [−3.0]
11	**X4**	5′-d(CGC ATA **X**TC GC)-3′	(−1)	44.5	48.5	51.0
	X2	3′-d(GCG TA**X** AAG CG)-5′		(−1.0) [−1.0]	(+3.0) [+7.5]	(+5.5) [−0.5]
12	**X3**	5′-d(CGC ATA T**X**C GC)-3′	(−2)	50.5	40.5	50.0
	X2	3′-d(GCG TA**X** AAG CG)-5′		(+5.0) [+3.5]	(−5.0) [+2.5]	(+4.5) [+1.5]
13	**X4**	5′-d(CGC ATA **X**TC GC)-3′	(−3)	37.5	17.5	47.0
	X1	3′-d(GCG **X**AT AAG CG)-5′		(−8.0) [−8.0]	(−28.0) [−14.5]	(+1.5) [+0.5]
14	**X3**	5′-d(CGC ATA T**X**C GC)-3′	(−4)	46.0	19.0	44.0
	X1	3′-d(GCG **X**AT AAG CG)-5′		(+0.5) [−1.0]	(−26.5) [−10.5]	(−1.5) [+0.5]

[a]Melting temperatures obtained from the maxima of the first derivatives of the melting curves (A_{260} vs temperature) recorded in a buffer containing 2.5 mM Na_2HPO_4, 5.0 mM NaH_2PO_4, 100 mM NaCl, 0.1 mM EDTA, pH 7.0, using 1.0 μM concentrations of each strand. **K**, **L**, and **M** correspond to the incorporation of the amidites **4**, **7**, and **11**, respectively. [b]Differences in melting temperatures as compared to the unmodified duplexes; $\Delta T_m = T_{m(duplex)} - T_{m(T1:T2)}$. [c]Differences in melting temperatures as compared to singly modified duplexes; $\Delta\Delta T_m = \Delta T_{m(a:b)} - (\Delta T_{m(a:T2)} + \Delta T_{m(T1:b)})$.

Table 2. Hybridization Data for Regular and Bulged DNA:DNA and DNA:RNA Duplexes

	complement	**X8** = 5′- d(GCT CAC **X**CT CCC A), T_m/°C,[a] (ΔT_{m1}/°C[b]), [ΔT_{m2}/°C[c]]				
		X = T	**X = TT**	**X = K**	**X = L**	**X = M**
DNA	3′- d(CGA GTG AGA GGG T)	52.5	Nd	54.5 (+2.0)	48.5 (−4.0)	56.5 (+3.5)
RNA	3′- r(CGA GUG AGA GGG U)	61.0	Nd	58.0 (−3.0)	56.5 (−4.5)	60.0 (−1.0)
DNA, A-bulge	3′- d(CGA GTG AAG AGG GT)	43.0	53.5	52.5 (+9.5) [−1.0]	43.5 (+0.5) [−10.0]	55.0 (+12.0) [+2.0]
RNA, A-bulge	3′- r(CGA GUG AAG AGG GU)	50.5	60.5	54.5 (+4.0) [−6.0]	54.0 (+3.5) [−6.5]	55.0 (+5.0) [−5.0]
DNA, GA-bulge	3′- d(CGA GTG AGA GAG GGT)	43.5	42.5	48.5 (+5.0) [+6.0]	43.0 (−0.5) [+0.5]	47.0 (+3.5) [+4.5]
RNA, GA-bulge	3′- r(CGA GUG AGA GAG GGU)	50.5	50.5	51.0 (+0.5) [+0.5]	52.5 (+2.0) [+2.0]	52.0 (+2.0) [+2.0]

[a]Melting temperatures obtained from the maxima of the first derivatives of the melting curves (A_{260} vs temperature) recorded in a buffer containing 2.5 mM Na_2HPO_4, 5.0 mM NaH_2PO_4, 100 mM NaCl, 0.1 mM EDTA, pH 7.0, using 1.0 μM concentrations of each strand. **K**, **L**, and **M** correspond to the incorporation of the amidites **4**, **7**, and **11**, respectively. [b]Differences in melting temperatures as compared to **X** = T. [c]Differences in melting temperatures as compared to **X** = TT.

and **M** in the same ON's gave the sequences **K1**−**K7**, **L1**−**L7**, and **M1**−**M7** (Table 1). These sequences were first mixed with unmodified complementary sequences, and the melting temperatures (T_m) of these modified duplexes were recorded by UV spectroscopy (Table 1, entries 2−8) and compared with the T_m of the corresponding unmodified duplex (entry 1). Hereby, the differences in melting temperature (ΔT_m's) were determined (Table 1). For the monomer **K**, ΔT_m's in the range of −1.0 to +1.5 °C were observed, indicating that all single and double incorporations of monomer **K** are well accommodated in dsDNA. For the monomer **L**, it is clear from the observed ΔT_m values (Table 1) that single or double incorporation gives a significant destabilization of the duplexes formed, and the largest decreases were seen for the modifications toward the 3′-end of the duplexes (entries 2 and 4). However, when monomer **L** was incorporated exactly in the middle of the sequence, no destabilization of the duplex was observed (entry 3). These results are well in accordance with the independent study on monomer **L**.[19] Similar destabilization of modified duplexes was observed with monomers **G** and **H** having an additional nucleobase on the triazole ring in place of the pyrene,[5] suggesting the triazole attached directly to the 2′-

dx.doi.org/10.1021/jo301571s | J. Org. Chem. 2012, 77, 9562−9573

Table 3. Hybridization Data for Three-Way Junctions

		T_m /°C[a] (ΔT_m /°C[b])			
		DNA hairpin: 3′- d(CGA GTG A CC CGC GTT TTC GCG AGA GGG T)		RNA hairpin: 3′- r(CGA GUG A CG CGU UUU CGC G AG AGG GU)	
ON	sequence	$[Mg^{2+}]$, 0 mM	$[Mg^{2+}]$, 10 mM	$[Mg^{2+}]$, 0 mM	$[Mg^{2+}]$, 10 mM
T	5′-d(GCT CAC TCT CCC A)-3′	24.5	38.0	37.0	47.0
K8	5′-d(GCT CAC **K**CT CCC A)-3′	43.5 (+19.0)	52.5 (+14.5)	43.5 (+6.5)	51.0 (+4.0)
L8	5′-d(GCT CAC **L**CT CCC A)-3′	33.5 (+9.0)	43.0 (+5.0)	44.0 (+7.0)	52.5 (+5.5)
M8	5′-d(GCT CAC **M**CT CCC A)-3′	38.0 (+14.0)	47.5 (+9.0)	48.5 (+11.5)	57.5 (+10.5)
TT	5′-d(GCT CAC TTC TCC CA)-3	26.0	38.5	37.5	47.5
KK	5′-d(GCT CAC **KK**C TCC CA)-3′	47.5 (+21.5)	54.5 (+16.0)	46.0 (+8.5)	54.0 (+6.5)
LL	5′-d(GCT CAC **LL**C TCC CA)-3′	37.0 (+11.0)	46.0 (+7.5)	48.5 (+11.0)	56.5 (+9.0)
MM	5′-d(GCT CAC **MM**C TCC CA)-3′	39.5 (+13.5)	49.5 (+10.5)	49.5 (+12.0)	59.0 (+11.5)
KL	5′-d(GCT CAC **KL**C TCC CA)-3′	36.0 (+10.0)	45.0 (+6.5)	43.0 (+5.5)	53.5 (+6.0)
LK	5′-d(GCT CAC **LK**C TCC CA)-3′	47.0 (+21.0)	54.0 (+15.5)	49.0 (+11.5)	58.0 (+10.5)
MK	5′-d(GCT CAC **MK**C TCC CA)-3′	48.0 (+22.0)	54.5 (+16.0)	50.5 (+13.0)	59.0 (+11.5)

[a]Melting temperatures obtained from the maxima of the first derivatives of the melting curves (A_{260} vs temperature) recorded in a buffer containing 2.5 mM Na_2HPO_4, 5.0 mM NaH_2PO_4, 100 mM NaCl, 0.1 mM EDTA, pH 7.0, using 1.0 μM concentrations of each strand. **K**, **L**, and **M** correspond to the incorporation of the amidites **4**, **7**, and **11**, respectively. [b]Differences in melting temperatures as compared to **X** = T.

position of the 2′-deoxyuridine as the primary destabilizing factor. Monomer **M**, in general, induced an increase in the duplex stability, suggesting that a flexible methylene linker between the 2′-position of the 2′-deoxyuridine and triazole ring is crucial for the stability of the modified duplex (compare data for monomers **L** and **M**). Nevertheless, neutral or negative influence on the duplex stability was observed when monomer **M** was placed near to the 3′-end in an ON sequence (entries 2 and 4).

Hereafter, the modified sequences were mixed to study the possibility for zipper contacts between the same modifications (**K**, **L**, or **M**) in the minor groove or to reveal the possibility for intercalation of the pyrene into the duplex. Hence, the two modifications in each of the complementary strands were placed with 0−3 interspacing base pairs, revealing possible (+1) to (−4) zippers as shown in Table 1. When the modified sequences **K2** and **K5** were mixed, to form a so-called (+1) zipper arrangement, the resulting duplex was found to be thermally more stable than either of the two duplexes with just one modification (compare entry 9 with entries 3 and 6), suggesting a favorable zipper contact ($\Delta\Delta T_m$ = +7.0 °C) between two pyrenes from opposite strands. An energetically unfavorable contact between the pyrene moieties with two modifications in a (−3) zipper motif (entry 13, $\Delta\Delta T_m$ = −8.0 °C) was observed, which is completely opposite to what was found for monomer **B** in the same arrangement.[3,4] For the remaining zippers (entries 10, 11, 12, and 14) no specific contacts were indicated, as the $\Delta\Delta T_m$ values are small.

For monomer **L**, a relative increase in the thermal stability of the (−1) zipper duplexes (Table 1, entries 10 and 11, large positive $\Delta\Delta T_m$'s) suggested a stabilizing contact between 2′-substitiuents. An energetically unfavorable zipper interaction was observed for monomer **L** in a (+1) zipper contact (entry 9, $\Delta\Delta T_m$ = −6.5 °C). Highly unstable duplexes were observed in the (−3) and (−4) zipper motifs with monomer **L** (entries 13 and 14). However, it is important to note that these duplexes are modified with monomer **L** close to 3′-end in each strand, where monomer **L** induced largest destabilization of the duplex (entries 2 and 4).

Monomer **M** in a (+1) zipper arrangement induced significant destabilization of the zipper duplex (ΔT_m = −6.0 °C and $\Delta\Delta T_m$ = −16.0 °C, entry 9). This could indicate a sterical interaction, for instance a simultaneous intercalation of the two pyrene units leading to the local unwinding of the duplex, thereby causing a decrease in thermal stability as reported previously for other ON's modified with intercalating pyrene moieties in a (+1) zipper arrangement.[23] However, another possibility could be a contact between two pyrene units in the minor groove away from the duplex core thereby disturbing hydration of the duplex leading to a thermally unstable duplex. In all other cases (entries 10−14) very stable duplexes were formed, but no zipper contacts were observed for monomer **M** as indicated by very neutral values of $\Delta\Delta T_m$ in the range of −3.0 °C to +1.5 °C.

Finally, also the zipper arrangements with more than two pyrenes in the duplex as obtained by using the sequences **X6**−**X7** were studied. For results and discussion, see Supporting Information.

To study the effect of the monomers **K**, **L**, and **M** in different bulged duplexes and three-way junctions, three 13-mer sequences with the monomer placed in the central position, **K8**, **L8**, and **M8**, were prepared and mixed with different complementary strands (Table 2). First, a standard duplex formed with a fully matched DNA sequence was studied. An increase in the thermal stability of the modified duplex was observed for monomers **K** and **M** compared to the unmodified duplex (ΔT_m = 2.0 and 3.5 °C, respectively), whereas monomer **L** led to the destabilization of the modified duplex by 4.0 °C compared to the unmodified duplex. These data are in line with the observations from Table 1. Upon hybridization with an RNA complement, all the monomers led to a destabilization of the corresponding DNA:RNA duplex. However, monomer **M** was found to be the best tolerated with a ΔT_m of −1.0 °C.

Hereafter, we investigated the hybridization of the modified 13-mer sequences with complementary bulged DNA and RNA sequences, that is 14- or 15-mer sequences with one or two unpaired nucleotides. When placed opposite to the bulged adenine monomers, **K** and **M** induced large increases in the thermal stability of a DNA:DNA duplex compared to an unmodified bulged duplex (ΔT_m = +9.5 °C and +12.0 °C, respectively, Table 2). Moreover, thermal stability of the modifed duplexes was found to be comparable to that of a regular duplex (i.e., with two thymidines instead of **K** or **M**).

dx.doi.org/10.1021/jo301571s | J. Org. Chem. 2012, 77, 9562−9573

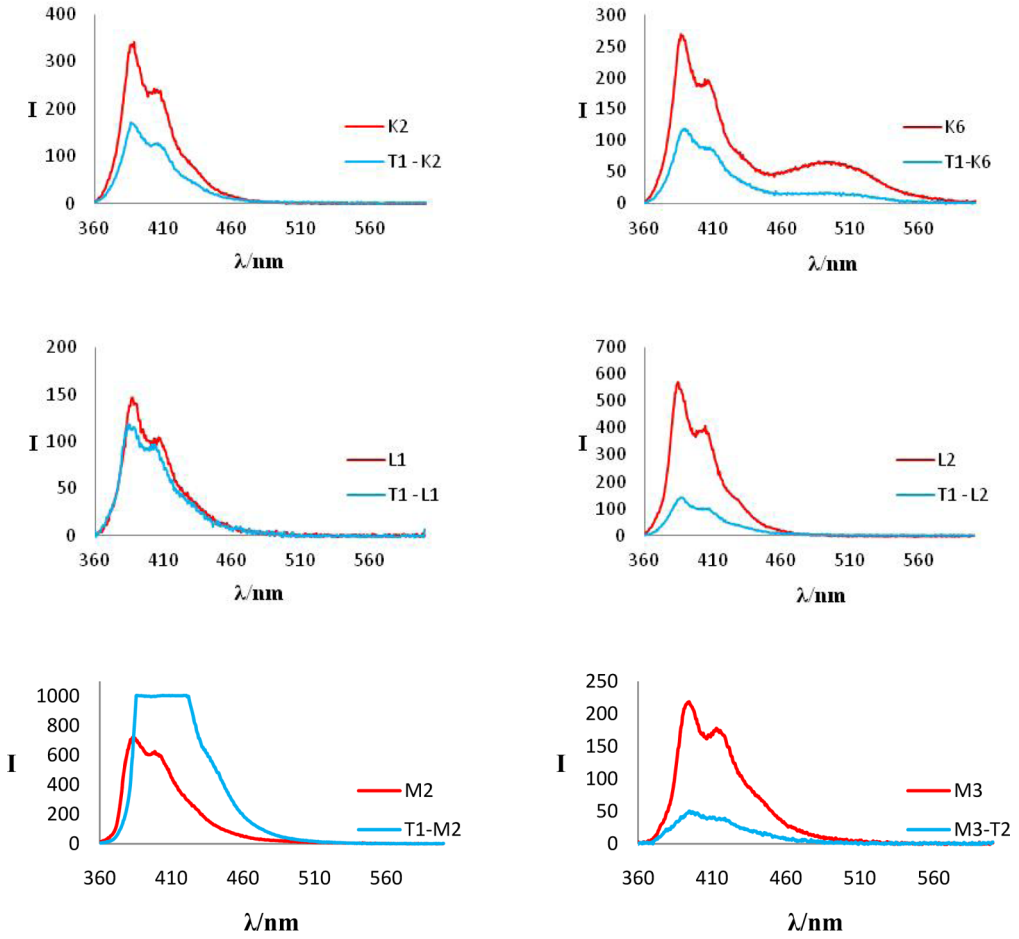

Figure 2. Representative steady-state fluorescence emission spectra for modified ON's (**K2**, **K6**, **L1**, **L2**, **M2**, and **M3**) in the absence (red) and presence (blue) of complementary DNA (λ_{ex} = 350 nm; T = 10 °C; [ON] = 1.0 μM). Different scaling of the Y-axes is used. For the remaining ON's, and full spectra of **T1**-**M2** ([ON] = 0.25 μM), see Figures S1−S4 (Supporting Information).

This suggests a favorable stacking interaction of the additional pyrene from monomer **K** or **M** into the bulge. However, for a DNA:DNA duplex having an adenine bulge opposite to monomer **L**, no change in the thermal stability was observed when compared to an unmodified A-bulge DNA duplex. A significant but smaller stabilization of the corresponding DNA:RNA bulged duplex (ΔT_m = +4.0 °C and +5.0 °C, respectively) was also observed for monomer **K** or **M**. Interestingly, for a DNA:RNA duplex, monomer **L** was found to stabilize the modified duplex by 3.5 °C. When studied in GA-bulged duplexes, the monomers, in general, were found to induce smaller stabilizations of the modified duplexes compared to the unmodified duplex.

Next, ON's **K8**, **L8**, and **M8** were mixed with DNA and RNA strands with standard stable hairpin sequences flanked by single-stranded regions being complementary to the modified sequences. Hereby, the effect of additional pyrenes at the branching point of TWJ's was studied (Table 3). The DNA hairpin complement used in this study contains an additional CC-bulge compared to the RNA complement to form a well-defined secondary structure.[24] As evident from Table 3, monomer **K** was found to have a very large stabilizing effect on the modified TWJ with ΔT_m = +19.0 °C as compared to that of the unmodified TWJ with thymidine in place of monomer **K**, suggesting favorable stacking interactions from the large aromatic surface of pyrene with nucleobases from one of the three stems of the TWJ. Monomers **L** and **M** demonstrated smaller but significant increases in the thermal stability of the corresponding TWJ (ΔT_m = +9.0 °C and +14.0 °C, respectively). A comparison of monomers **L** and **M** revealed that introduction of the flexible methylene linker between the triazole moiety and the 2′-carbon has a favorable effect on the stability of the TWJ in accordance with that observed for the regular duplexes (Table 1). Nevertheless, the results for monomer **K** suggested that the 5′-(*S*)-C position is placing pyrene in a better position for stacking interactions with neighboring nucleobases than the 2′-position. In comparison, monomer **M** was found to have the largest stabilizing effect in regular duplexes. The stabilizing effect of monomer **K** was found to be significantly reduced when studied in a DNA:RNA TWJ. However, for monomers **L** and **M**, the effect on the stability of the DNA:RNA TWJ was found to be comparable to that on the stability of the DNA:DNA TWJ. Upon addition of Mg^{2+} to the complexes, the stability of the TWJ increases significantly in all the studied cases, but the relative stabilization effect of the modifications decreases slightly.

Finally, six 14-mer sequences with two consecutive incorporations of the same or different monomers (**KK**, **LL**, **MM**, **KL**, **LK**, and **MK**) were synthesized to study the presence of an additional pyrene in the branching point of the TWJ (Table 3). The idea was that the two pyrenes might interact to stabilize the complexes and/or form fluorescent probes (vide

dx.doi.org/10.1021/jo301571s | J. Org. Chem. 2012, 77, 9562−9573

infra). Before studying TWJ's, the modified sequences were mixed with regularly matched DNA or RNA strands and, in all cases, small to medium decreases in the thermal stability were observed (Table S3, Supporting Information), ΔT_m's between −1.5 °C and −8.5 °C). Next, these modified ON's were mixed with DNA and RNA strands with the standard stable hairpin sequences (Table 3). The two adjacent incorporations of either of the monomers **K**, **L**, or **M** in the branching points induced large increases in the thermal stability of the resulting duplex compared to the unmodified sequence with two thymidines in place of the modified monomers. The highest increase (ΔT_m = +21.5 °C) was observed for monomer **K** (ON **KK**) in line with the single incorporation of monomer **K** (ON **K8**). However, when compared to the effect of the first modification in a 13-mer sequence (ON's **K8**, **L8**, and **M8**), the effect of introducing an extra pyrene monomer into the TWJ was found to be small. Interestingly, with two different monomers at the branching point, thermal stability of the complex with monomer **L** toward the 5′-end and monomer **K** toward the 3′-end (ON **LK**) was found to be significantly higher than that of the opposite arrangement of monomers (ON **KL**), indicating possible favorable contact between the two pyrenes from the different monomers in the former arrangement. This is in line with the large stabilizing effect observed with ON **MK** in the TWJ (ΔT_m = +22.0 °C). In the DNA:RNA TWJ, the relative stability induced by two **K** monomers was found to be significantly less than that observed in DNA:DNA TWJ context while monomers **L** and **M** do not show any preference for a DNA hairpin complement over a RNA hairpin complement in parallel to data obtained for ON's **L8** and **M8**. ON's **LK** and **MK** also showed a relative preference for a DNA hairpin over an RNA hairpin complement similar to ON **KK**. As observed earlier for ON's **K8**, **L8**, and **M8**, the addition of Mg^{2+} led to increases of the TWJ stability in all cases, but the relative stabilization effect of the modifications decreases slightly.

Fluorescence Studies. We recorded the steady-state fluorescence emission spectra of all the 11-mer sequences modified with monomers **K**, **L**, and **M** in the absence and presence of unmodified and modified complementary DNA (see sequences in Table 1) at 10 °C by exciting pyrene at 350 nm. For all single-stranded ON's containing monomer **K**, two well-defined bands for the pyrene monomer fluorescence (λ_{max} ∼387 and ∼406 nm) were observed (Figures 2 and S1 (Supporting Information)). Upon hybridization with the complementary DNA sequence, a decrease in the fluorescence emission intensity was observed, indicating an intercalation of the pyrene into the duplex where its fluorescence is quenched by the neighboring bases. A broad pyrene−pyrene excimer band at λ_{max} = ∼490 nm was obtained for the ON's **K6** and **K7** with two incorporations of the pyrenes at alternate positions (Figure 2 and S1), suggesting the close proximity of two pyrenes in the single-stranded probes. Near complete disappearance of the excimer signal along with the decrease in the intensity of pyrene monomer fluorescence upon hybridization with the DNA complement indicated the intercalation of one or both of the pyrene units.

For monomer **L** (Figures 2 and S2 (Supporting Information)), no significant change in the fluorescence intensity upon hybridization was observed except when placed centrally in the duplex (ON **L2**), which displayed a large decrease in the fluorescence intensity (compare **L2** and **T1:L2**, Figure 2). It is important to note that ON **L2** induced no thermal destabilization of the corresponding duplex **T1:L2** in contrast to all other ON's incorporated with monomer **L** (Table 1). In a different sequence context studying monomer **L**, a decrease in the fluorescence quantum yield upon hybridization with complementary DNA has been observed,[19] suggesting the intercalation of the pyrene into the duplex. Thermal denaturation data (Table 1) in combination with steady-state fluorescence spectra for monomer **L** suggested the intercalation of the pyrene toward the 3′-direction, which may cause local unwinding of the duplex when present near the 3′-end, accounting for the destabilization of the duplex in such cases.

Fluorescence emission intensity for ON's **M1**−**M5** was also found to be dependent on the sequence (Figures 2 and S3 (Supporting Information)). Single-stranded ON's with an A**M**A context (**M2** and **M5**) were found to be highly fluorescent as compared to the other ON's (**M1**, **M3**, and **M4**), strengthening the fact that adenine is the weakest quencher of the pyrene fluorescence.[25,26] In general, a large increase in the fluorescence intensity upon hybridization with a complementary DNA strand was observed for ON's modified with monomer **M**, which indicates the positioning of the pyrene unit into the minor groove away from the duplex core. However, when placed close to the 3′-end (ON's **M1** and **M3**), the corresponding modified duplexes (**T1**:**M1** and **M3**:**T2**) were found to be significantly less fluorescent.

Hereafter, steady-state fluorescence emission spectra of all interstrand zippers (see Table 1) were recorded. The emission spectra of all the studied zipper duplexes for monomers **K**, **L**, and **M** displayed structured pyrene emission bands with λ_{max} in the range of 385−391 nm and 404−409 nm (Figure 3). When monomer **K** was placed in a (−1) zipper arrangement in modified duplexes (**K5**:**K1** and **K4**:**K2**), a pyrene excimer signal with λ_{max} = ∼490 nm was observed as a broad shoulder, suggesting the close proximity of two pyrene units from monomer **K** in opposite strands. DNA duplexes with more than two incorporations of monomer **K** in general displayed broad bands corresponding to the pyrene excimer fluorescence signal (Figure S6 (Supporting Information)).

An excimer band with only very low fluorescence intensity was observed when monomer **L** was placed in a (−1) zipper arrangement in modified duplexes (**L5**:**L1** and **L4**:**L2**) (Figure 3). This supports the T_m data for this arrangement, which showed favorable interaction between two additional pyrene units from opposite strands (Table 1), but it is not clear how this is structured. The intensity of this excimer signal increases in the presence of an additional pyrene in the modified duplexes (Figure S6).

Zippers of monomer **M** (Figures 3 and S6) showed the same very strong intensities as observed for the single modified duplexes (Figures 2 and S3). For monomer **M**, the presence of an excimer band in a (+1) zipper arrangement (**M5**:**M2**) further strengthens our hypothesis of close contact between two pyrene units as the cause for relatively low thermal stability (Table 1). This specific (+1) zipper contact between two pyrene units of monomer **M** from opposite strands was found to be undisturbed by the presence of additional pyrene units in the modified duplex as indicated by the steady-state fluorescence spectra of multizippers (Figure S6).

Steady-state fluorescence spectra of 13-mer sequences (**K8**, **L8**, and **M8**) were measured in the absence and presence of matched DNA or RNA targets (Figure S8 (Supporting Information)). A hybridization-induced decrease in pyrene monomer fluorescence was observed for monomer **K** upon mixing ON **K8** with DNA or RNA complement, strengthening

dx.doi.org/10.1021/jo301571s | J. Org. Chem. 2012, 77, 9562−9573

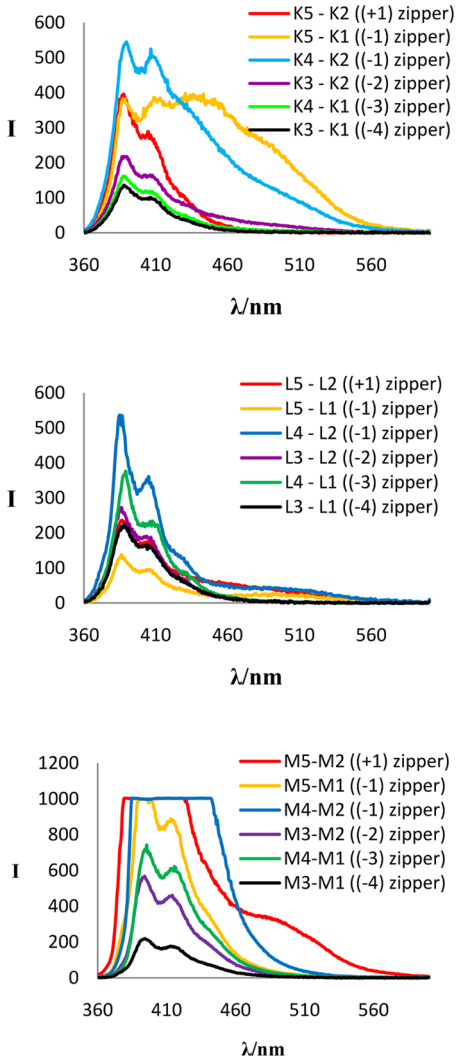

Figure 3. Steady-state fluorescence emission spectra of interstrand zippers (Table 1) (λ_{ex} = 350 nm; T = 10 °C; [ON] = 1.0 μM). Different scaling of the Y-axes is used. For full spectra of duplexes **M5-M2** and **M4-M2** ([ON] = 0.25 μM) see Figure S5 (Supporting Information).

our hypothesis of intercalation of pyrene from monomer **K** into the duplex. Monomer **L** displayed a large increase in the fluorescence intensity upon hybridization with the matched RNA target compared to single-stranded probe **L8**, while against complementary DNA no significant change in the fluorescence intensity was observed upon hybridization. This suggested that pyrene is pointing away from the base stack into the minor groove of the DNA:RNA duplex while it is at least partly intercalated with neighboring bases in the DNA:DNA duplex. For monomer **M** (ON **M8**), no significant change in the steady-state fluorescence spectra was observed upon hybridization with complementary RNA, whereas an increase in fluorescence intensity was again seen with DNA target.

Thereafter, steady-state fluorescence spectra of sequences **K8**, **L8**, and **M8** were recorded in the presence of complementary bulged DNA or RNA sequences, or DNA or RNA strands with hairpin sequences forming TWJ's (Figure S8). In general, relatively low fluorescence intensity of the pyrene in the corresponding bulged duplexes with additional adenine in the complementary strand was observed, indicating intercalation of the pyrene. This is in line with the large increase in the thermal stability of these modified duplexes compared to unmodified bulged duplexes (Table 2). When introduced into TWJ's, all pyrene monomers (**K**, **L**, and **M**) displayed only small changes in the fluorescence intensity.

Finally, the six 14-mer sequences with two adjacent incorporations of the same or different monomers in the middle of the sequence were investigated (Figure 4). Steady-state fluorescence spectra of the single-stranded 14-mer sequence with two adjacent incorporations of monomer **K** or **L** (ON's **KK** and **LL**, Table 3) displayed the typical two bands (λ_{max} = ∼386 nm and ∼406 nm) for pyrene monomer fluorescence along with a pyrene−pyrene excimer band with λ_{max} = ∼490 nm of low intensity. However, the corresponding sequence **MM** displayed an intense unstructured band with λ_{max} = ∼480 nm for the excimer signal along with very intense bands for pyrene monomer fluorescence (λ_{max} = ∼384 nm and ∼403 nm). Upon hybridization with fully matched DNA or RNA sequences, ON **KK**, and to some extent **LL**, displayed increases in the fluorescence bands as well as a significant increase of the excimer signal (Figure 4). From these results it can be concluded that both pyrenes are pointing into the minor groove away from the duplex core and are able to interact with each other. ON **MM** displayed a decrease in the fluorescence emission intensity of the pyrene monomer bands and a complete disappearance of the excimer signal upon hybridization with the DNA complement (Figure 4). This indicates intercalation of at least one of the pyrenes into the duplex. However, against the RNA complement, ON **MM** displayed an intense but somewhat red-shifted excimer signal. This indicated that in a DNA:RNA duplex, the two pyrenes are in close proximity to each other to form an excimer signal, making this probe a promising candidate for the selective detection of single-stranded RNA over single-stranded DNA. This difference in excimer formation between dsDNA and DNA:RNA might be due to structurally different minor grooves.

Next, the 14-mer sequences with two adjacent incorporations of different monomers were studied. ON **LK** (see Table 3) displayed a very weak and broad band for pyrene excimer fluorescence (Figure 4). When mixed with the RNA complement, ON **LK** displayed an intense band at λ_{max} = ∼450 nm with a broad shoulder starting at ∼475 nm, which can be assigned to the pyrene−pyrene excimer signal. However, against the matched DNA sequence, a very broad band with center at λ_{max} = ∼480 nm was found. ON **KL** failed to display the excimer signal in its steady-state fluorescence spectrum also upon hybridization with complementary DNA. Upon hybridization with the RNA complement, a very weak excimer signal was observed. This could be attributed to the large distance between the two pyrenes (pointing in opposite directions) in the single-stranded probe and in the corresponding modified duplexes. For sequence **MK**, an intense excimer signal was observed in the single-stranded form as well as upon hybridization with DNA or RNA sequences.

Finally, steady-state fluorescence spectra of all the 14-mer sequences were recorded in the presence of standard stable hairpin sequences forming TWJ's (Figure 4). ON **KK** displayed a weak and broad excimer signal upon mixing with the RNA hairpin complement. However, no such excimer formation was observed against the DNA hairpin complement, suggesting that the formation of excimer is selective for the RNA hairpin complement, but the very low intensity of this signal probably makes it unsuitable for any diagnostic application. ON **LL** displayed a weak excimer signal upon hybridization with the

dx.doi.org/10.1021/jo301571s | J. Org. Chem. 2012, 77, 9562−9573

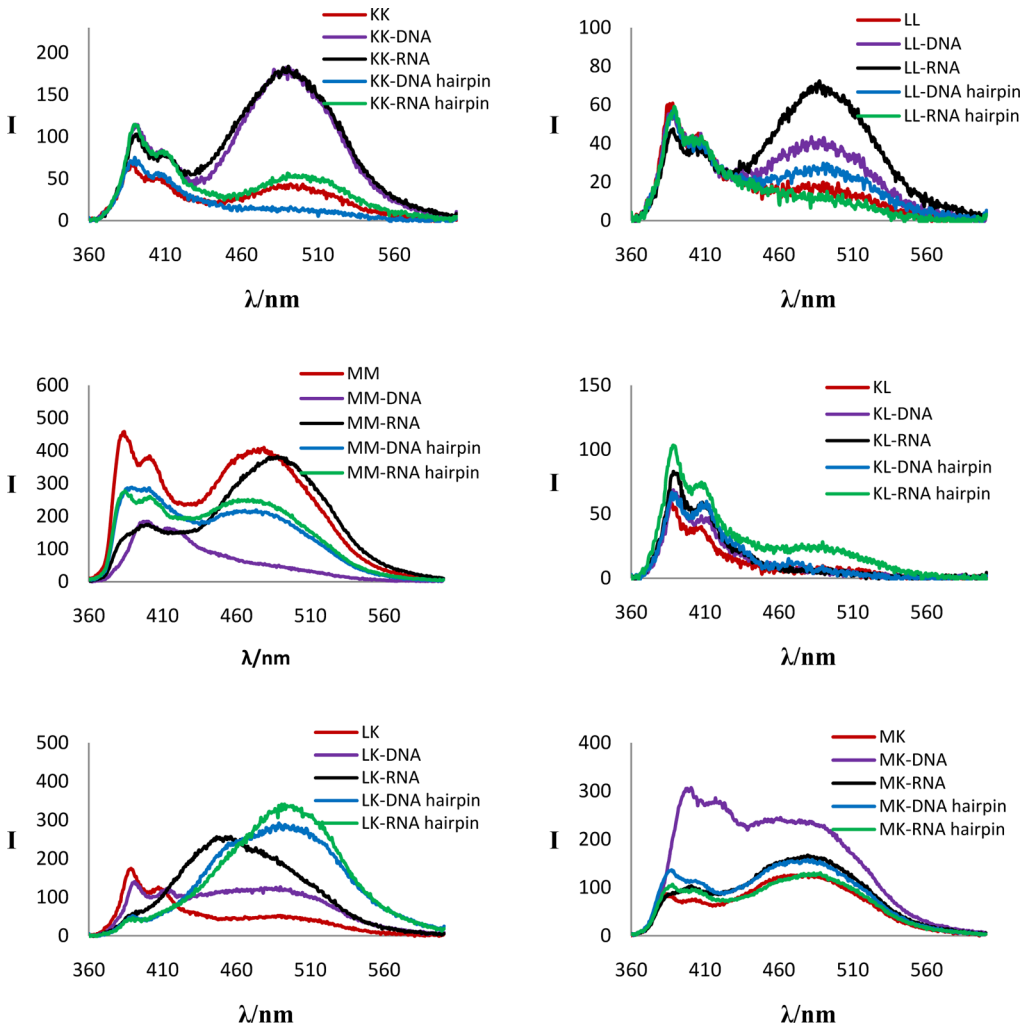

Figure 4. Steady-state fluorescence emission spectra of modified single-stranded 14-mer ON's (**KK**, **LL**, **MM**, **KL**, **LK**, **MK**) and their duplexes with complementary DNA or RNA sequence, and standard stable hairpin sequences flanked by single-stranded regions being complementary to the modified sequences (λ_{ex} = 350 nm; T = 10 °C ; [ON] = 1.0 μM). Different scaling of Y-axes is used.

DNA or RNA hairpin complements. ON **MM** displayed an excimer formation upon mixing with DNA or RNA hairpin complements, however, with decreased intensity as compared to the single-stranded probe **MM**. As no excimer formation was observed for ON **MM** against a regular DNA complement, ON **MM** has a potential to discriminate between a DNA hairpin and a regular DNA complement. Interestingly, ON **LK** displayed an intense unstructured excimer signal against the DNA/RNA hairpin complements, whereas in the opposite arrangement of the monomers, ON **KL** failed to show any excimer signal. ON **MK** also displayed excimer signals against the hairpin complements, however, also in the single-stranded states and in the duplexes.

DISCUSSION

In the following, the hybridization and subsequent fluorescence properties of the three monomers are summarized:

Monomer K. On the basis of the general decrease in fluorescence intensity upon hybridization, the 5′-position for the pyrene moiety of **K** seems in favor of intercalation into the duplex. The intercalation might be situated between the first and the second unmodified base-pair in the 5′-direction to the modified nucleotide as justified by the fact that specifically only the (−3) zipper orientation of two monomers in the complementary strands leads to a significant decrease in duplex stability. Hence, the two pyrenes cannot intercalate into the same space in the duplex, and indeed no excimer band has been observed. A decrease in fluorescence intensity indicated intercalation of the pyrene also in the DNA:RNA duplex. The introduction of monomer **K** into bulged duplexes or TWJ's leads to strong increases in stability, more so in DNA:DNA than in DNA:RNA complexes, probably in connection to aromatic stacking in the complexes as validated by small decreases in fluorescent intensity upon hybridization.

Monomer L. In general, incorporation of this monomer into duplexes leads to decreases in thermal stability as compared to unmodified duplexes. The general destabilization might be a result of the rather inflexible structure with the triazole connected directly to the C-2′ of the ribose and thereby a sterical conflict in the duplex core. In another study similar decreases in duplex stability have been observed for **L**.[19] In general, fluorescence intensity decreases upon hybridization, indicating that the pyrene moiety at least partly intercalates into the duplex. In contrast to the DNA:DNA duplexes, the pyrene of **L** seems not to intercalate into the DNA:RNA duplex, as a huge increase in fluorescence is seen upon hybridization. In bulged duplexes, this picture changes as **L** leads to an increase

dx.doi.org/10.1021/jo301571s | J. Org. Chem. 2012, 77, 9562−9573

in stability, especially of the bulged DNA:RNA complex followed by a small decrease in fluorescence, indicating intercalation into the bulge. This stabilizing effect is not seen with the bulged DNA:DNA. Also the TWJ's were stabilized by **L**, but whereas the effect is smaller than with **K** for the DNA:DNA complex, it is slightly larger for the DNA:RNA complex.

Monomer M. In contrast to monomer **L**, the incorporation of **M** into duplexes generally leads to stabilized duplexes. This might be due to the flexibility inserted by a methylene linker between the triazole and C2′. In general, the stabilized duplexes are followed by very large increases in fluorescence intensity, whereas the few neutral or destabilized duplexes are followed by decreases in fluorescence intensity. This clearly indicates that the sequence contexts have a large influence and that the pyrene moiety in general seems to be positioned in the minor groove without intercalation. Two or more incorporations of monomer **M** were found to be well tolerated in an 11-mer dsDNA, suggesting that formation of heavily modified duplexes is a possibility with monomer **M**. Unfavorable interaction between the substituents in the (+1) zipper structure is indicated by fluorescence as well as by T_m. Monomer **M** is also found to stabilize the bulged duplexes, and in the case of a single nucleotide A-bulge, this is followed by relative decreases in fluorescence intensity, indicating that intercalation takes place in the bulges. Also the TWJ's are significantly stabilized, apparently as a consequence of stacking as justified from decreases in fluorescence.

Fluorescent Probes for Hybridization. The double-modified sequences (Table 3) are all found to stabilize the TWJ's significantly, which is of course interesting from a targeting aspect. Nevertheless, equally interesting is the diversity in fluorescence, and especially excimer formation, upon formation of the complexes (duplexes or TWJ's), indicating the potential of these ON's as recognition probes. Hence, **MM** displays a strong excimer band as a single strand and in a DNA:RNA duplex but not in a DNA:DNA duplex. This makes **MM** a potential probe for RNA over DNA complements. As might be expected from the structures, **LK** with the two pyrenes positioned toward each other is much more interesting than **KL**. **LK** demonstrates large excimers when complexed with hairpins as compared to its duplexes, and it might function as a probe for hairpins. Finally, **KK** forms large excimers in both DNA:DNA and DNA:RNA duplexes and much smaller excimers with hairpins. Hereby, **KK** acts exactly opposite to that of **LK** as a probe for single-stranded complements over hairpins. **MK** does not show the same potential as **LK** because excimer bands are formed in all complexes as well as in the single strand.

In summary, interesting properties have been found for all the three monomers **K**, **L**, and **M**, and all have the potential to find application in the targeting of nucleic acid sequences or in diagnostic probes. From a perspective of targeting DNA or RNA, it is very interesting that the pyrene monomers can lead to the formation of very stable TWJ's due to aromatic stacking. When compared to the corresponding double-headed nucleosides (Figure 1), it is clear that the pyrene-modified monomers **K**, **L**, and **M** demonstrate completely different properties. For instance, **K** has the opposite tendency to that of monomer **B**, as **K** leads to a destabilized (−3) zipper complex. Whereas the pyrene of **K** intercalates into the duplex, the thymine of **B** (and of **C**) interacts in the minor groove. In general, this study of pyrene analogues of double-headed nucleotides has shown that the constitution, for instance the aromatic surface, rather than the position of the substituent dictates the behavior in duplexes and TWJ's. Compared to other pyrene-containing nucleotides described in the literature, there are differences and similarities. Monomer **M** behaves differently when compared to other 2′-modified analogues, such as 2′-OCH$_2$Pyr or 2′-N(CH$_3$)-CH$_2$Pyr.[14,27] These have shown a strong tendency to intercalate in DNA:DNA duplexes, whereas this does not seem to be the case for **M**. This might be due to local conformational differences around the modified monomers, as also indicated by the fact that monomer **L** is more prone to intercalation than **M**.

CONCLUSION

We have described efficient synthetic access to three new pyrene-modified nucleotides. These have shown interesting properties in the formation of synthetic nucleic acid complexes with varying fluorescence emission. Monomer **K** forms stable duplexes with the pyrene moiety intercalating in a predictable way. Monomer **L** leads to somewhat distorted and destabilized duplexes with the pyrene intercalated, whereas monomer **M** leads to stabilized duplexes with the pyrene situated in the minor groove. All three monomers can lead to significant stabilization of bulged duplexes and TWJ's, overall with **K** > **M** > **L** in DNA:DNA complexes and **M** > **K** > **L** in DNA:RNA complexes. Interesting excimer formation in combination with stabilized TWJ's is observed with two adjacent monomers **LK**, whereas interesting excimer formation in duplexes is observed for **KK** and for **MM**, the latter for DNA:DNA duplexes making it only a probe for DNA over RNA. The study demonstrates that pyrene-modified nucleotides can have various applications as diagnostic probes and in nucleic acid targeting and that the positioning of the pyrene moiety is delicate and crucial for the structural output.

EXPERIMENTAL SECTION

General. All commercial reagents were used as supplied, except CH$_2$Cl$_2$ which was distilled prior to use. Anhydrous solvents were dried over 4 Å activated molecular sieves (CH$_2$Cl$_2$, DMF, pyridine, and DCE) or 3 Å activated molecular sieves (CH$_3$CN). All reactions were carried out under an atmosphere of argon or nitrogen, when using anhydrous solvents. Reactions were monitored using TLC analysis with Merck silica gel plates (60 F$_{254}$). To visualize the plates, they were exposed to UV light (254 nm) and/or immersed in a solution of 5% H$_2$SO$_4$ in methanol followed by charring. Standard column chromatography was performed using silica gel 60 (0.040−0.063 mm). ^{1}H NMR, ^{13}C NMR, and ^{31}P NMR spectra were recorded at 400, 101, and 162 MHz, respectively. Chemical shift values (δ) are reported in ppm relative to either tetramethylsilane (^{1}H NMR) or the deuterated solvents as internal standard for ^{13}C NMR (δ: CDCl$_3$ 77.16 ppm, DMSO-d_6 39.52 ppm) and relative to 85% H$_3$PO$_4$ as external standard for ^{31}P NMR. 2D spectra (^{1}H−^{1}H COSY and ^{1}H−^{13}C HSQC) have been used in assigning ^{1}H and ^{13}C NMR signals. High resolution ESI (quadrupole) mass spectra were recorded in positive mode.

3′-*O*-(*tert*-Butyldimethylsilyl)-5′-*O*-pixyl-5′(*S*)-*C*-[(4-(pyren-1-yl)-1,2,3-triazol-1-yl)methyl]thymidine (2). To a solution of compound **1**[4] (500 mg, 0.75 mmol) and 1-ethynylpyrene (226 mg, 1.00 mmol) in THF:H$_2$O:pyridine (12 mL, 5:5:2 v/v) were added sodium ascorbate (37 mg, 0.19 mmol) and CuSO$_4$·5H$_2$O (25 mg, 0.10 mmol), and the solution was stirred at room temperature overnight. Additional sodium ascorbate (37 mg, 0.19 mmol) and CuSO$_4$·5H$_2$O (25 mg, 0.10 mmol) were added, and the reaction mixture was stirred for another 3 h at room temperature. To the mixture was added CH$_2$Cl$_2$ (40 mL), and it was washed with a 10% aqueous solution of NaHCO$_3$ (30 mL). The aqueous phase was extracted with CH$_2$Cl$_2$ (3 × 40 mL), and the combined organic phase was dried (Na$_2$SO$_4$) and

dx.doi.org/10.1021/jo301571s | J. Org. Chem. 2012, 77, 9562−9573

concentrated under reduced pressure. The residue was purified by column chromatography (1−3% MeOH in CH_2Cl_2), affording the product **2** (564 mg, 84%) as a yellow foam. R_f 0.36 (5% MeOH in CH_2Cl_2); ^{1}H NMR (300 MHz, $CDCl_3$) δ 8.55 (d, J = 9.6 Hz, 2H, Ar), 8.21−7.99 (m, 8H, Ar, NH), 7.82 (d, 1H, J = 0.6 Hz, H6), 7.67 (s, 1H, H5-triazole), 7.52−7.33 (m, 9H, Ar), 7.25−7.03 (m, 4H, Ar), 6.24 (dd, 1H, J = 5.1, 9.6 Hz, H1′), 4.16 (dd, 1H, J = 8.8, 13.0 Hz, H6′), 3.91−3.80 (m, 2H, H5′, H6′), 3.48 (s, 1H, H4′), 3.35 (d, J = 4.8 Hz, 1H, H3′), 2.05 (s, 3H, CH_3), 2.00 (m, 1H, H2′), 1.91 (m, 1H, H2′), 0.68 (s, 9H, $(CH_3)_3$), −0.19 (s, 3H, CH_3Si), −0.29 (s, 3H, CH_3Si); ^{13}C NMR (75 MHz, $CDCl_3$) δ 163.7 (C4), 152.2, 152.0 (Ar), 150.3 (C2), 147.4 (C4-triazole), 146.2 (Ar), 135.7 (C6), 131.5, 131.4, 131.0, 130.9, 130.7, 130.5, 128.2, 128.1, 128.0, 127.8, 127.7, 127.4, 127.1, 126.2, 125.5, 125.5, 125.2, 125.1, 124.9, 124.8, 124.7, 124.2, 124.1, 124.0, 122.9, 122.5, 117.6, 117.2 (Ar + C5-triazole), 111.2 (C5), 86.8 (C4′), 84.9 (C1′), 78.9 (C-Ar_3), 73.2 (C3′), 72.2 (C5′), 50.3 (C6′), 41.0 (C2′), 25.7 ($(CH_3)_3$), 17.7 (CSi), 12.8 (CH_3), −4.5, −4.7 (CH_3Si); HR-ESI MS m/z 916.3504 ([M + Na]$^+$, $C_{54}H_{51}N_5O_6SiNa^+$ calcd 916.3501).

5′-*O*-Pixyl-5′(*S*)-*C*-[(4-(pyren-1-yl)-1,2,3-triazol-1-yl)methyl]-thymidine (3). Nucleoside **2** (373 mg, 0.42 mmol) was dissolved in anhydrous THF (6.0 mL), and a 1.0 M solution of TBAF in THF (0.42 mL, 0.42 mmol) was added. The reaction mixture was stirred for 3 h at room temperature. CH_2Cl_2 (20 mL) was added, and the resulting solution was washed with a saturated aqueous solution of $NaHCO_3$ (15 mL). The aqueous phase was extracted with CH_2Cl_2 (3 × 10 mL), and the combined organic phases were washed with water (20 mL), dried (Na_2SO_4), and concentrated under reduced pressure. The residue was purified by column chromatography (0−10% MeOH, 0.5% pyridine in CH_2Cl_2) to afford the product **3** (267 mg, 82%) as a light yellow foam; R_f 0.56 (10% MeOH in CH_2Cl_2); ^{1}H NMR (400 MHz, $CDCl_3$) δ 8.59 (d, 1H. J = 9.3 Hz, Ar), 8.51 (s, 1H, NH), 8.24−7.99 (m, 8H, Ar), 7.66 (s, 1H, H5-triazole), 7.56−7.00 (m, 14H, H6, Ar), 6.13 (t, 1H, J = 6.6 Hz, H1′), 4.19 (m, 1H, H6′), 4.03 (m, 1H, H6′), 3.92 (m, 1H, H5′), 3.73 (m, 1H, H3′), 3.50 (t, 1H, J = 4.2 Hz, 1H, H4′), 2.26−2.06 (m, 3H, 3′−OH, H2′), 2.00 (s, 3H, CH_3); ^{13}C NMR (101 MHz, $CDCl_3$) δ 163.6 (C4), 152.2, 152.1 (Ar), 150.2 (C2), 147.6 (C4-triazole), 146.5 (Ar), 136.1 (C6), 131.6, 131.40, 131.38 131.0, 130.8, 130.5, 128.6, 128.4, 128.2, 128.1, 127.7, 127.5, 127.2, 126.3, 125.7, 125.4, 125.2, 125.1, 125.0, 124.9, 124.7, 124.4, 124.2, 123.8, 122.8, 122.7, 117.5, 117.0 (Ar, C5-triazole), 111.4 (C5), 85.0 (C4′), 84.2 (C1′), 78.4 (C-Ar_3), 71.4 (C4′), 70.2 (C3′), 50.5 (C6′), 40.1 (C2′), 12.9 (CH_3). HR-ESI MS m/z 802.2642 ([M + Na]$^+$, $C_{48}H_{37}N_5O_6Na^+$ calcd 802.2637).

3′-*O*-(2-Cyanoethoxy-*N*,*N*-diisopropylaminophosphinyl)-5′-*O*-pixyl-5′(*S*)-*C*-[(4-(pyren-1-yl)-1,2,3-triazol-1-yl)methyl]-thymidine (4). To a solution of **3** (300 mg, 039 mmol) in anhydrous CH_2Cl_2 (4 mL) were added *N*,*N*-diisopropylethylamine (0.26 mL, 1.50 mmol) and 2-cyanoethyl-*N*,*N*-diisopropylamino chlorophosphite (0.20 mL, 0.90 mmol) under Ar atmosphere. The reaction mixture was stirred at room temperature for 2 h. CH_2Cl_2 (30 mL) was added, and the mixture was washed with a 10% aqueous solution of $NaHCO_3$. The aqueous phase was extracted with CH_2Cl_2 (3 × 30 mL), and the combined organic phase was dried (Na_2SO_4) and concentrated under reduced pressure. The residue was purified by column chromatography (0−20% $(CH_3)_2CO$, 0.25% pyridine in CH_2Cl_2) to give the product **4** (260 mg, 69%) as a yellow foam: R_f 0.27, 0.36 (10% $(CH_3)_2CO$ in CH_2Cl_2); ^{31}P NMR (162 MHz, $CDCl_3$) δ 151.61, 151.47; HR-ESI MS m/z 1002.3718 ([M + Na]$^+$, $C_{57}H_{54}N_7O_7PNa^+$ calcd 1002.3714).

5′-*O*-(4,4′-Dimethoxytrityl)-2′-(4-(pyren-1-yl)-1,2,3-triazole-1-yl)-2′-deoxyuridine (6). Nucleoside **5** (102 mg, 0.18 mmol), 1-ethynylpyrene (51 mg, 0.23 mmol), and TBTA (17 mg, 0.05 mmol) were dissolved in a mixture of THF:H_2O:pyridine (6:3:2, 1.7 mL), and the solution was degassed under argon. A solution of sodium ascorbate (14 mg, 0.07 mmol) and $CuSO_4 \cdot 5H_2O$ (9 mg, 0.04 mmol) in water (0.25 mL) was added, and the reaction mixture was stirred at room temperature for 24 h. The reaction mixture was diluted with CH_2Cl_2 (15 mL), and the mixture was washed with a saturated aqueous solution of $NaHCO_3$ (10 mL). The aqueous phase was extracted with CH_2Cl_2 (3 × 10 mL). The combined organic phases were dried (Na_2SO_4) and concentrated under reduced pressure. The residue was purified by column chromatography (50−100% EtOAc, 0.5% pyridine in petroleum ether) to afford the product **6** (112 mg, 79%) as a yellow foam; R_f 0.36 (5% MeOH in CH_2Cl_2); ^{1}H NMR (400 MHz, $CDCl_3$) δ 8.78 (s, 1H, NH), 8.32 (d, 1H, J = 9.3 Hz, pyrene), 8.16 (s, 1H, H5-triazole), 8.10−7.74 (m, 9H, pyrene, H6), 7.44−7.13 (m, 9H, DMT), 6.84 (d, 4H, J = 8.6 Hz, DMT), 6.43 (d, 1H, J = 5.3 Hz, H1′), 5.36 (d, 1H, J = 8.2 Hz, H5), 5.25 (t, 1H, J = 5.7 Hz, H2′), 4.90 (dd, 1H, J = 5.9, 11.8 Hz, H3′), 4.53 (m, 1H, H4′), 4.21 (3′−OH), 3.78 (s, 6H, OCH_3), 3.56 (m, 2H, H5′); ^{13}C NMR (101 MHz, $CDCl_3$) δ 162.7 (C4), 158.99, 158.97 (DMT), 150.4 (C2), 147.4 (C4-triazole), 144.4 (DMT), 139.4 (C6), 135.3, 135.1 (DMT), 131.5, 131.3, 130.7, 130.32, 130.27, 128.42, 128.38, 128.1, 127.4, 127.3, 127.0, 126.1, 125.5, 125.3, 124.94, 124.90, 124.87, 124.5, 124.2, 124.1 (DMT, pyrene, C5-triazole), 113.6 (DMT), 103.2 (C5), 87.6 (C-Ph_3), 87.0 (C1′), 84.8 (C4′), 71.0 (C3′), 66.6 (C2′), 62.4 (C5′), 55.4 (OCH_3). HRMS-ESI: m/z 798.2948 ([M + H]$^+$, $C_{48}H_{39}N_5O_7H^+$ calcd 798.2922).

3′-*O*-(2-Cyanoethoxy-*N*,*N*-diisopropylaminophosphinyl)-5′-*O*-(4,4′-dimethoxytrityl)-2′-(4-(pyren-1-yl)-1,2,3-triazole-1-yl)-2′-deoxyuridine (7). Nucleoside **6** (184 mg, 0.23 mmol) was coevaporated twice with anhydrous DCE and dissolved in the same solvent (4.0 mL). *N*,*N*-Diisopropylethylamine (0.41 mL, 2.35 mmol) and 2-cyanoethyl-*N*,*N*-diisopropylamino chlorophosphite (0.11 mL, 0.49 mmol) were added, and the reaction mixture was stirred at room temperature for 4 h. Ethanol (1.5 mL) and CH_2Cl_2 (20 mL) were added, and the solution was washed with a saturated aqueous solution of $NaHCO_3$ (15 mL). The aqueous phase was extracted with CH_2Cl_2 (2 × 10 mL), and the combined organic phases were dried (Na_2SO_4) and concentrated under reduced pressure. The residue was purified by column chromatography (0−100% EtOAc, 0.5% pyridine in petroleum ether). The residue was precipitated three times from a solution in EtOAc (1.5 mL) poured into cold petroleum ether (70 mL) to afford the product **7** (111 mg, 48%) as a light yellow foam; R_f 0.59 (5% MeOH in CH_2Cl_2); ^{31}P NMR (162 MHz, $CDCl_3$) δ 151.8, 150.2 (3:2). HRMS-ESI: m/z: 1020.3857 ([M + Na]$^+$, $C_{57}H_{56}N_7O_8PNa^+$ calcd 1020.3821).

5′-*O*-(4,4′-Dimethoxytrityl)-2′-*C*-(prop-2-yn-1-yl)-2′-deoxyuridine (9). Nucleoside **8**[20] (165 mg, 0.62 mmol) was coevaporated with anhydrous pyridine (2 × 5 mL) and redissolved in the same solvent (10 mL). 4,4′-Dimethoxytrityl chloride (270 mg, 0.80 mmol) was added, and the reaction mixture was stirred at room temperature for 16 h. Ethanol (1.0 mL) was added, and the mixture was concentrated under reduced pressure. The residue was dissolved in CH_2Cl_2 (20 mL), and the mixture was washed with a saturated aqueous solution of $NaHCO_3$ (2 × 15 mL). The combined aqueous phase was extracted with CH_2Cl_2 (2 × 15 mL), and the combined organic phase was dried (Na_2SO_4), concentrated under reduced pressure, and coevaporated with a mixture of toluene and EtOH (15 mL, 1:2, v/v). The residue was purified by column chromatography (0−5% MeOH in CH_2Cl_2, v/v) to afford the product **9** (280 mg, 79%) as a slightly yellow solid. R_f 0.5 (5% MeOH in CH_2Cl_2); ^{1}H NMR (400 MHz, DMSO-d_6) δ 11.32 (br s, 1H, NH), 7.53 (d, 1H, J = 8.4 Hz, H6), 7.40−7.24 (m, 9H, Ar), 6.92−6.89 (m, 4H, Ar), 5.92 (d, 1H, J = 8.0 Hz, H1′), 5.50 (d, 1H, J = 5.2 Hz, 3′−OH), 5.47 (d, 1H, J = 8.4 Hz, H5), 4.19 (m, 1H, H3′), 4.14 (m, 1H, H4′), 3.74 (s, 6H, OCH_3), 3.25 (dd, 1H, J = 4.4, 10.0 Hz, H5′), 3.15 (dd, 1H, J = 4.4, 10.0 Hz, H5′), 2.78 (t, 1H, J = 2.4 Hz, C≡CH), 2.48−2.41 (m, 2H, H2′, CH_2), 2.23 (m, 1H, CH_2); ^{13}C NMR (100 MHz, DMSO-d_6) δ 162.8 (C4), 158.0 (DMT), 150.6 (C2), 144.5 (C6), 140.2, 135.2, 135.1, 129.6, 130.2, 127.8, 127.5, 126.6, 113.1 (DMT), 101.8 (C5), 86.8 (C1′), 85.8 (CPh$_3$), 84.9 (C4′), 81.7 (C≡CH), 71.5 (C3′), 71.4 (C≡CH), 63.7 (C5′), 54.9 (OCH_3), 45.9 (C2′), 13.6 (CH_2C≡CH); HRMS-ESI: m/z: 591.2094 ([M + Na]$^+$, $C_{33}H_{32}N_2O_7Na^+$ calcd 591.2107).

5′-*O*-(4,4′-Dimethoxytrityl)-2′-(1-(pyren-1-yl)-1,2,3-triazole-4-yl)methyl)-2′-deoxyuridine (10). Nucleoside **9** (100 mg, 0.17 mmol) was dissolved in THF:H_2O:*t*BuOH (10 mL, 3:1:1, v/v/v). To the solution was added an aqueous solution of sodium ascorbate (1 M, 0.6 mL, 0.6 mmol), an aqueous solution of $CuSO_4$ (0.6 mL, 7.5% w/v, 0.17 mmol), and 1-azidopyrene (100 mg, 0.40 mmol). The mixture

dx.doi.org/10.1021/jo301571s | J. Org. Chem. 2012, 77, 9562−9573

was stirred at room temperature for 2 h was and then diluted with EtOAc (20 mL) and brine (20 mL). The phases were separated, and the organic phase was washed with a saturated aqueous solution of $NaHCO_3$ (20 mL). The combined aqueous phase was extracted with EtOAc (2 × 10 mL), and the combined organic phase was dried (Na_2SO_4) and concentrated under reduced pressure. The residue was purified by column chromatography (0−4% MeOH in CH_2Cl_2) to afford the product **10** (90 mg, 63%) as a yellowish green solid. R_f 0.4 (80% EtOAc in petroleum ether); ^{1}H NMR (400 MHz, $CDCl_3$) δ 8.88 (br s, 1H, NH), 8.27 (d, J = 7.8 Hz, 1H, Ar), 8.24 (d, J = 8.2 Hz, 1H, Ar), 8.21 (d, J = 7.8 Hz, 1H, Ar), 8.17 (d, J = 8.8 Hz, 1H, Ar), 8.11 (d, J = 8.8 Hz, 1H, Ar), 8.10−8.03 (m, 2H, Ar), 8.02 (d, J = 8.0 Hz, 1H, Ar).7.92 (s, 1H, H5-triazole), 7.77 (d, 1H, J = 8.0 Hz, Ar), 7.75 (d, 1H, J = 8.0 Hz, Ar), 7.41−7.39 (m, 2H, Ar), 7.31−7.28 (m, 6H, Ar, H6), 7.23−7.20 (m, 2H, Ar, H6), 6.83 (d, 4H, J = 8.8 Hz, Ar), 6.25 (d, 1H, J = 8.0 Hz, H1′), 5.85 (d, 1H, J = 8.8 Hz, H5), 4.64−4.61 (m, 2H, OH, H3′), 4.29 (m, 1H, H4′), 3.75 (s, 6H, OCH_3), 3.53−3.50 (m, 2H, H5′), 3.35 (dd, 1H, J = 14.6, 10.0 Hz, CH_2), 3.07 (dd, 1H, J = 14.6, 4.4 Hz, CH_2), 2.72 (m, 1H, H2′); ^{13}C NMR (100 MHz, $CDCl_3$) δ 162.8 (C4), 158.7 (DMT), 150.6 (C2), 145.0, 144.4, 140.2, 135.4, 135.3, 132.3, 131.1, 130.5, 130.1, 130.0, 129.9, 129.0, 128.1, 128.0, 127.1, 126.9, 126.8, 126.5, 126.1, 126.0, 125.0, 124.8, 124.7, 124.1, 123.2, 120.7, 113.3 (DMT, pyrene, C6), 102.7 (C5), 88.2, 86.9 (*C*-Ph_3, C1′), 85.6 (C4′), 73.1 (C3′), 64.0 (C5′), 55.2 (OCH_3), 51.0 (C2′), 20.9 (CH_2); HR ESI MS m/z 834.2902 ($[M + Na]^+$, $C_{49}H_{41}N_5O_7Na^+$ calcd 834.2898).

3′-*O*-(2-Cyanoethyl-*N*,*N*-diisopropylaminophosphinyl)-5′-*O*-(4,4′-dimethoxytrityl)-2′-(1-(pyren-1-yl)-1,2,3-triazole-4-yl)-methyl)-2′-deoxyuridine (11). Nucleoside **10** (180 mg, 0.22 mmol) was coevaporated twice with anhydrous DCE and dissolved in anhydrous CH_2Cl_2 (5.0 mL). *N*,*N*-Diisopropylethylamine (0.20 mL, 1.14 mmol) and 2-cyanoethyl-*N*,*N*-diisopropylamino chlorophosphite (80 μL, 0.33 mmol) were added, and the reaction mixture was stirred at room temperature for 1 h. Ethanol (0.2 mL) and CH_2Cl_2 (15 mL) were added, and the resulting solution was washed with a saturated aqueous solution of $NaHCO_3$ (15 mL). The aqueous phase was extracted with CH_2Cl_2 (2 × 10 mL), and the combined organic phases were dried (Na_2SO_4) and concentrated under reduced pressure. The residue was purified by column chromatography (0−2% MeOH in CH_2Cl_2) to afford the product **11** (145 mg, 64%) as a light yellow foam; R_f 0.50 (3% MeOH in CH_2Cl_2); ^{31}P NMR (162 MHz, $CDCl_3$) δ 150.5, 149.3. HRMS-ESI m/z 1034.3953 ($[M + Na]^+$ $C_{58}H_{58}N_7O_8PNa^+$ calcd 1034.3977).

Oligonucleotide Synthesis. Oligonucleotide synthesis was carried out on an automated DNA synthesizer following the phosphoramidite approach. Synthesis of oligonucleotides **K1−8**, **L1−8**, **M1−8**, **KK**, **LL**, **MM**, **MK**, **LK**, and **KL** were performed on a 0.2 μmol scale (CPG support) by using the modified nucleoside phosphoramidites **4**, **7**, and **11** to introduce monomers **K**, **L**, and **M**, respectively, as well as the corresponding commercial 2-cyanoethyl phosphoramidites of the natural 2′-deoxynucleosides. The synthesis followed the regular protocol for the DNA synthesizer. For the modified phosphoramidites, a prolonged coupling time of 20 min was used. 1*H*-Tetrazole was used as activator. In general, coupling yields for all 2-cyanoethyl phosphoramidites were >80%. The 5′-*O*-DMT-ON oligonucleotides were removed from the solid support by treatment with concentrated aqueous ammonia at 55 °C for 12 h. The oligonucleotides were purified by reversed-phase HPLC on a C18 10 μm; 7.8 × 150 mm column + precolumn: C18 10 μm, 7.8 × 10 mm. Buffer A: 0.05 M triethyl ammonium acetate, pH 7.4. Buffer B: 75% MeCN/H_2O (3:1, v/v). Program used: 2 min 100% A, 100−30% A over 38 min, 10 min 100% B, 10 min 100% A. All oligonucleotides were detritylated by treatment with 80% aqueous acetic acid for 20 min and neutralized by addition of sodium acetate (3 M, 15 μL), and then sodium perchlorate (5 M, 15 μL) was added followed by acetone (1 mL). The pure oligonucleotides precipitated overnight at −20 °C. The mixture was then placed in a centrifuge and subjected to 12 000 rpm for 10 min at 4 °C. The supernatant was removed and the pellet washed with cold acetone (2 × 1 mL). The pellet was then dried for 30 min under reduced pressure and dissolved in pure water (1 mL), and the concentration was measured as OD 260 nm. The purity and constitution of the ON's were confirmed by IC analysis and MALDI-TOF MS $[M - H]^+$, respectively (Table S1).

Thermal Denaturation Experiments. Samples were dissolved in a medium salt buffer containing 2.5 mM Na_2HPO_4, 5 mM NaH_2PO_4, 100 mM NaCl, and 0.1 mM EDTA at pH = 7.0 with 1.0 μM concentrations of the two complementary oligonucleotide sequences. The increase in UV absorbance at 260 nm as a function of time was recorded while the temperature was increased linearly from 10 °C to 80 °C at a rate of 1.0 °C/min by means of a Peltier temperature programmer. The melting curves were found to be reversible. All determinations are averages of at least duplicates within ±0.5 °C. For melting experiments with Mg^{2+} concentrations of 10 mM, $MgCl_2$ (2.0 μL of a 5.0 M solution) was added to the samples.

Fluorescence Experiments. Fluorescence spectra (360−600 nm) were recorded using quartz optical cells with a path length of 1.00 cm. The samples from the thermal denaturation experiments were reused for the fluorescence experiments. All samples were annealed at 75 °C prior to measurements. Background spectra were recorded and subtracted from all measurements. The spectra were recorded at 10 °C.

■ ASSOCIATED CONTENT

Ⓢ Supporting Information

MALDI-TOF data for oligonucleotides. Further thermal denaturation data and fluorescence spectra. Selected NMR spectra. This material is available free of charge via the Internet at http://pubs.acs.org.

■ AUTHOR INFORMATION

Corresponding Author

*Fax: +45 66158780. E-mail: pouln@sdu.dk.

Present Address

‡Department of Chemistry, University College, Kurukshetra University 136119, India.

Notes

The authors declare no competing financial interest.

■ ACKNOWLEDGMENTS

The project was supported by The Danish Research Agency's Programme for Young Researchers, Nucleic Acid Center and The Danish National Research Foundation, The Danish Councils for Independent Research | Technology and Production Sciences (FTP) and Natural Science (FNU), and The Villum Kann Rasmussen Foundation.

■ REFERENCES

(1) (a) Weisbrod, S. H.; Marx, A. *Chem. Commun.* **2008**, 5675−5685. (b) Gramlich, P. M. E.; Wirges, C. T.; Manetto, A.; Carell, T. *Angew. Chem., Int. Ed.* **2008**, *47*, 8350−8358. (c) Malinovskii, V. L.; Wenger, D.; Häner, R. *Chem. Soc. Rev.* **2010**, *39*, 410−422. (d) Bandy, T. J.; Brewer, A.; Burns, J. R.; Marth, G.; Nguyen, T.; Stulz, E. *Chem. Soc. Rev.* **2011**, *40*, 138−148.

(2) Tørring, T.; Voigt, N. V.; Nangreave, J.; Yan, H.; Gothelf, K. V. *Chem. Soc. Rev.* **2011**, *40*, 5636−5646.

(3) (a) Christensen, M. S.; Madsen, C. M.; Nielsen, P. *Org. Biomol. Chem.* **2007**, *5*, 1586−1594. (b) Andersen, C.; Sharma, P. K.; Christensen, M. S.; Steffansen, S. I.; Madsen, C. M.; Nielsen, P. *Org. Biomol. Chem.* **2008**, *6*, 3983−3988.

(4) Shaikh, K. I.; Madsen, C. S.; Nielsen, L. J.; Jørgensen, A. S.; Nielsen, H.; Petersen, M.; Nielsen, P. *Chem.—Eur. J.* **2010**, *16*, 12904−12919.

(5) Jørgensen, A. S.; Shaikh, K. I.; Enderlin, G.; Ivarsen, E.; Kumar, S.; Nielsen, P. *Org. Biomol. Chem.* **2011**, *9*, 1381−1388.

(6) Madsen, C. S.; Witzke, S.; Kumar, P.; Negi, K.; Sharma, P. K.; Petersen, M.; Nielsen, P. *Chem.—Eur. J.* **2012**, *18*, 7434−7442.

(7) (a) Pedersen, S. L.; Nielsen, P. *Org. Biomol. Chem.* **2005**, *3*, 3570−3575. (b) Christensen, M. S.; Bond, A.; Nielsen, P. *Org. Biomol. Chem.* **2008**, *6*, 81−91.
(8) (a) Wu, T.; Froeyen, M.; Schepers, G.; Mullens, K.; Rozenski, J.; Busson, R.; Van Aershot, A.; Herdewijn, P. *Org. Lett.* **2004**, *6*, 51−54. (b) Wu, T.; Nauwelaerts, K.; Van Aershot, A.; Froeyen, M.; Lescrinier, E.; Herdewijn, P. *J. Org. Chem.* **2006**, *71*, 5423−5431. (c) Umemoto, T.; Wengel, J.; Madsen, A. S. *Org. Biomol. Chem.* **2009**, *7*, 1793−1797. (d) Kielkowski, P.; Pohl, R.; Hocek, M. *J. Org. Chem.* **2011**, *76*, 3457−3462.
(9) (a) Tornøe, C. W.; Christensen, C.; Meldal, M. *J. Org. Chem.* **2002**, *67*, 3057−3064. (b) Rostovtsev, V. V.; Green, L. G.; Fokin, V. V.; Sharpless, K. B. *Angew. Chem., Int. Ed.* **2002**, *41*, 2596−2599.
(10) (a) Seela, F.; Ingale, S. A. *J. Org. Chem.* **2010**, *75*, 284−295. (b) Ingale, S. A.; Pujari, S. S.; Sirivolu, V. R.; Ding, P.; Xiong, H.; Mei, H.; Seela, F. *J. Org. Chem.* **2012**, *77*, 188−199.
(11) (a) Gramlich, P. M. E.; Wirges, C. T.; Manetto, A.; Carell, T. *Angew.Chem., Int. Ed.* **2008**, *47*, 8350−8358. (b) Amblard, F.; Cho, J. H.; Schinazi, R. F. *Chem. Rev.* **2009**, *109*, 4207−4220. (c) El-Sagheer, A. H.; Brown, T. *Chem. Soc. Rev.* **2010**, *39*, 1388−1405. (d) Østergaard, M. E.; Guenther, D. C.; Kumar, P.; Baral, B.; Deobald, L.; Paszczynski, A. J.; Sharma, P. K.; Hrdlicka, P. J. *Chem. Commun.* **2010**, *46*, 4929−4931.
(12) (a) Kocalka, P.; Andersen, N. K.; Jensen, F.; Nielsen, P. *ChemBioChem* **2007**, *8*, 2106−2116. (b) Andersen, N. K.; Chandak, N.; Brulikova, L.; Kumar, P.; Jensen, M. D.; Jensen, F.; Sharma, P. K.; Nielsen, P. *Bioorg. Med. Chem.* **2010**, *18*, 4702−4710. (c) Andersen, N. K.; Døssing, H.; Jensen, F.; Vester, B.; Nielsen, P. *J. Org. Chem.* **2011**, *76*, 6177−6187. (d) Kumar, P.; Chandak, N.; Nielsen, P.; Sharma, P. K. *Bioorg. Med. Chem.* **2012**, *20*, 3843−3849.
(13) (a) Okamoto, A.; Saito, Y.; Saito, I. *J. Photochem. Photobiol. C* **2005**, *6*, 108−122. (b) Malinovskii, V. L.; Wenger, D.; Häner, R. *Chem. Soc. Rev.* **2010**, *39*, 410−422.
(14) Østergaard, M. E.; Hrdlicka, P. J. *Chem. Soc. Rev.* **2011**, *40*, 5771−5788.
(15) Winnik, F. M. *Chem. Rev.* **1993**, *93*, 587−614.
(16) (a) Marti, A. A.; Jockusch, S.; Stevens, N.; Ju, J.; Turro, N. *J. Acc. Chem. Res.* **2007**, *40*, 402−409. (b) Kolpashchikov, D. M. *Chem. Rev.* **2010**, *110*, 4709−4723.
(17) (a) Abdel-Rahman, A. A.-H.; Ali, O. M.; Pedersen, E. B. *Tetrahedron* **1996**, *52*, 15311−15324. (b) Filichev, V.; Pedersen, E. B. *Org. Biomol. Chem.* **2003**, *1*, 100−103.
(18) (a) Kirschenheuter, G. P.; Zhai, Y.; Pieken, W. A. *Tetrahedron Lett.* **1994**, *35*, 8517−8520. (b) Catry, M. A.; Madder, A. *Molecules* **2007**, *12*, 114−129.
(19) Recently, the same monomer has been reported independently by Sau, S. P.; Hrdlicka, P. J. *J. Org. Chem.* **2012**, *77*, 5−16.
(20) Dreier, I.; Kumar, S.; Søndergaard, H.; Rasmussen, M. L.; Hansen, L. H.; List, N. H.; Kongsted, J.; Vester, B.; Nielsen, P. *J. Med. Chem.* **2012**, *55*, 2067−2077.
(21) Schrock, A. K.; Schuster, G. B. *J. Am. Chem. Soc.* **1984**, *106*, 5234−5240.
(22) (a) Børsting, P.; Nielsen, K. E.; Nielsen, P. *Org. Biomol. Chem.* **2005**, *3*, 2183−2190. (b) Sharma, P. K.; Mikkelsen, B. H.; Christensen, M. S.; Nielsen, K. E.; Kirchhoff, C.; Pedersen, S. L.; Sørensen, A. M.; Østergaard, K.; Petersen, M.; Nielsen, P. *Org. Biomol. Chem.* **2006**, *4*, 2433−2445.
(23) (a) Sau, S. P.; Kumar, T. S.; Hrdlicka, P. J. *Org. Biomol. Chem.* **2010**, *8*, 2028−2036. (b) Hrdlicka, P. J.; Kumar, T. S.; Wengel, J. *Chem. Commun.* **2005**, 4279−4281.
(24) Leontis, N. B.; Kwok, W.; Newman, J. S. *Nucleic Acids Res.* **1991**, *19*, 759−766.
(25) Østergaard, M. E.; Kumar, P.; Baral, B.; Guenther, D. C.; Anderson, B. A; Ytreberg, F. M.; Deobald, L.; Paszczynski, A. J.; Sharma, P. K.; Hrdlicka, P. J. *Chem.—Eur. J.* **2011**, *17*, 3157−3165.
(26) (a) Manoharan, M.; Tivel, K. L.; Zhao, M.; Nafisi, K.; Netzel, T. L. *J. Phys. Chem.* **1995**, *99*, 17461−1747. (b) Seo, Y. J.; Ryu, J. H.; Kim, B. H. *Org. Lett.* **2005**, *7*, 4931−4933.
(27) Karmakar, S.; Anderson, B. A.; Rathje, R. L.; Andersen, S.; Jensen, T. B.; Nielsen, P.; Hrdlicka, P. J. *J. Org. Chem.* **2011**, *76*, 7119−7131.